Electronic Supplementary Material (ESI) for Physical Chemistry Chemical Physics.

Supplementary Information

Ethanol, O, and CO adsorption on Pt nanoparticles: Effects of nanoparticle size and graphene support

L.G. Verga,[a] A.E. Russell,[a] and C-K. Skylaris[a*]

[a] Department of Chemistry, University of Southampton, Highfield, Southampton SO17 1BJ, United Kingdom

E-mail:* *c.skylaris@soton.ac.uk*

1 Adsorption energies and Generalized Coordination Number

Here, we show the correlation between the adsorption energies of O, CO, and ethanol and the generalized coordination numbers obtained for each adsorption site[1]. Figure 1, 2 and 3 present, respectively, the adsorption energies obtained for adsorbates interacting with bridge, hollow, and all the adsorption sites on (111) facets.

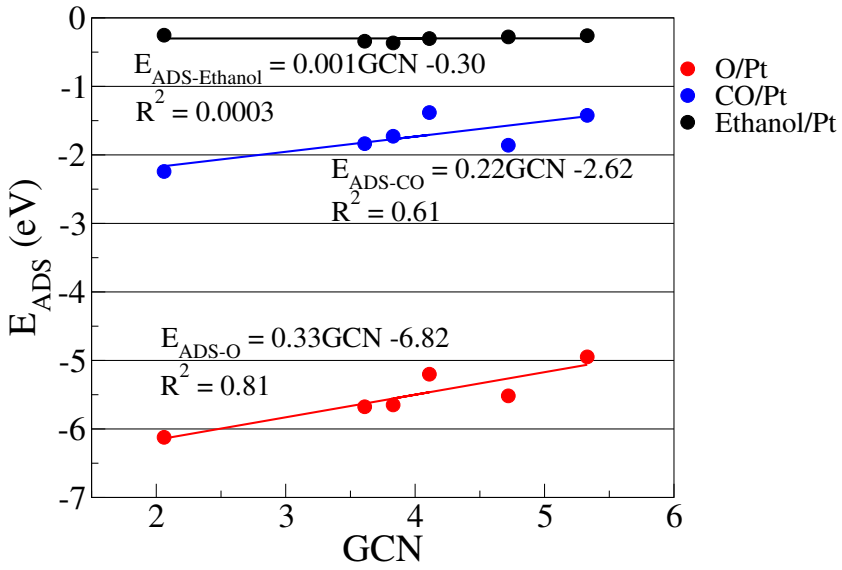

Figure 1 Adsorption energies for oxygen (red), carbon monoxide (blue), and ethanol (black) interacting with bridge sites on (111) facets versus the generalized coordination number relative to each adsorption site.

The general trend observed for bridge and hollow adsorption sites is similar to that found for top adsorption sites in the main article, with the generalized coordination number of a given adsorption site controlling the adsorption energies of O and CO to a greater extent than for ethanol. For oxygen adsorption, we obtained high correlation coefficients for all the cases, while for CO, adding hollow sites degraded the correlation between adsorption energies and the generalized coordination numbers.

For the ethanol adsorption, the slope of the linear equation and the correlation coefficient are considerably smaller for bridge and hollow sites as compared with the results for top sites in the main article. These findings are consistent with the results observed in the main article, with ethanol adsorption being favourable only on top sites and with the adsorption energies for bridge and hollow sites being dominated by dispersion interactions.

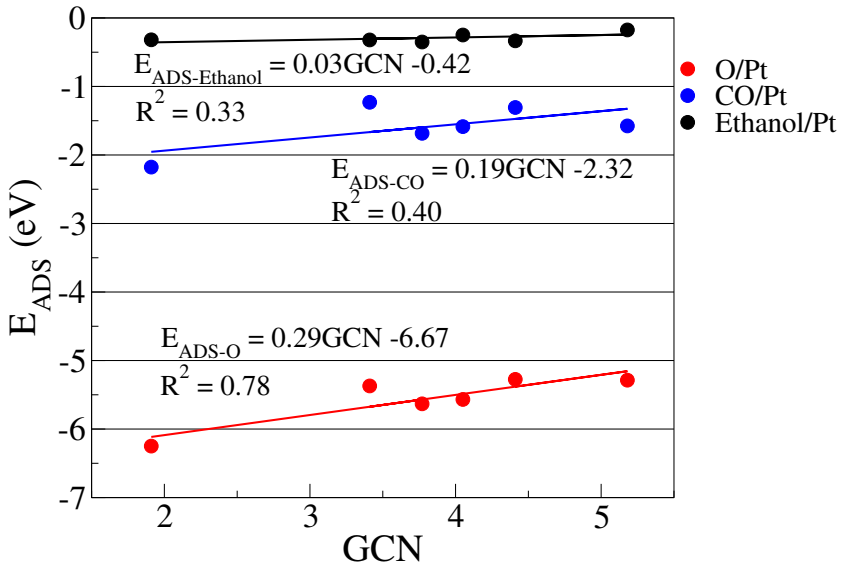

Figure 2 Adsorption energies for oxygen (red), carbon monoxide (blue), and ethanol (black) interacting with hollow sites on (111) facets versus the generalized coordination number relative to each adsorption site.

Presenting the correlation for the same type of adsorption sites for different nanoparticle sizes helps to illustrate how the nanoparticle size effects can be described to a certain extent via a purely geometrical descriptor. Correlations between adsorption energies and the generalized coordination numbers can also be useful as a predictive tool for catalyst activity in metallic nanoparticles and comparisons between our findings and previous results from the literature might be interesting in that context.

As an example, a recent work from Jørgessen *et al.*[2] obtained $E_{ADS-CO} = -1.36 + 0.252(GCN - 7.5)$ and $E_{ADS-O} = 0.95 + 0.218(GCN7.5)$. The differences between our results for the y-intercept and the ones obtained in the literature can be explained in terms of usage of different codes, exchange correlation functional and strategy to obtain the adsorption energies. The main differences in the y-intercept from our results and the ones from Jørgessen *et al.*[2] are observed for the O adsorption due to the different reference system used to calculate the adsorption energies. While we use an O atom as reference systems to calculate the adsorption energies, the authors use half of the energy of an O_2 molecule in the triplet state. Moreover, while we calculate the adsorption energies on rigid nanoparticles, the authors obtained their results on slab models, allowing two layers of Pt to relax during the interaction with the adsorbates, which can generate a constant shift compared to our results.

Meanwhile, the differences in the slopes are caused by the methodology used to choose the adsorption sites to obtain the linear correlations. In our work, we are using the same types of adsorption sites to obtain the correlations for each adsorbate. As discussed before, the motivation for that is showing the differences caused by size effects and not the differences between adsorption sites. Jørgessen *et al.* use the most stable adsorption site for each adsorbate on four different slab models. For CO, the authors use only top sites, and for O they use bridge sites on Pt(100), Pt(110), and Pt(211) and an FCC site for Pt(111).

Figure 1, 2 and 3 also show changes in the linear equations and correlation coefficients for each adsorbate depending on the type of adsorption site used to generate the correlation, indicating the need for careful parametrisation when using linear equations from generalized coordination number correlations to predict adsorption energies.

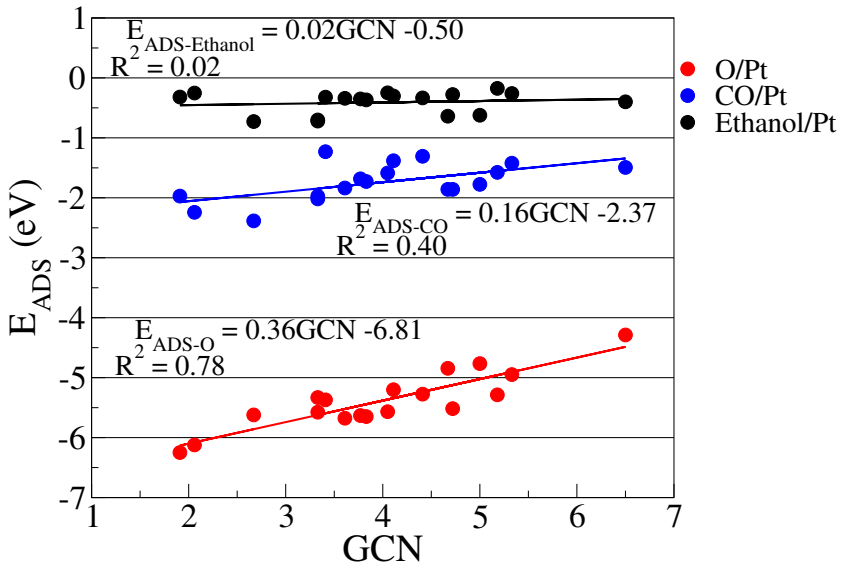

Figure 3 Adsorption energies for oxygen (red), carbon monoxide (blue), and ethanol (black) interacting with adsorption sites on (111) facets versus the generalized coordination number relative to each adsorption site.

2 Unrelaxed Pt nanoparticles

One of the effects associated with changes in the nanoparticle size is the change in Pt-Pt bond lengths. Changes in the bond lengths in the nanoparticle surface are associated with changes in the adsorption strength between nanoparticles and adsorbates. To assess the importance of these changes, we have calculated O, CO and ethanol adsorption on perfect cuboctahedral nanoparticles created with Pt-Pt bond lengths similar to those obtained for experimental Pt bulk, with a lattice parameter of 3.92 Å[3,4].

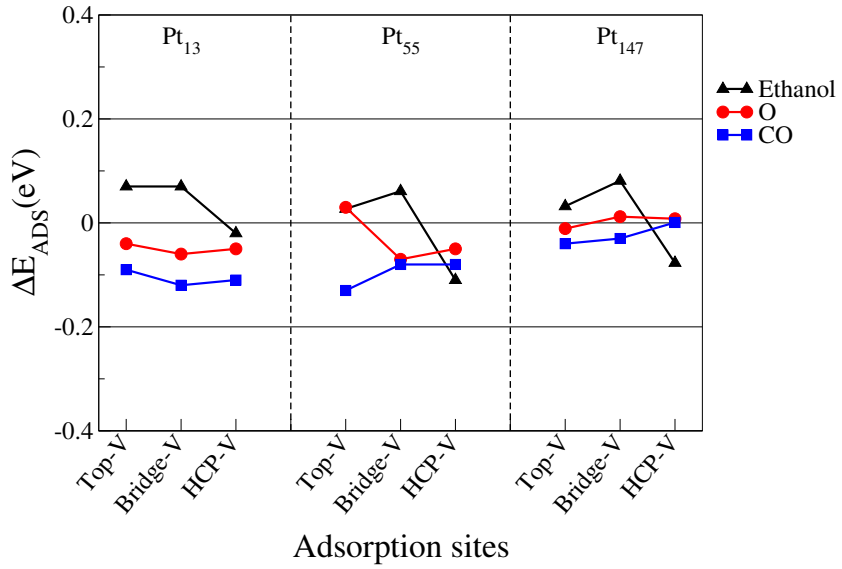

Figure 4 Differences in the adsorption energy of O, CO and ethanol interacting with Pt nanoparticle with bond lengths similar to those obtained for experimental Pt bulk and with fully optimised Pt nanoparticles. The letter V represents adsorption sites in the vertex of the nanoparticle facet.

Figure 4 shows the difference between adsorption energies obtained with perfect cuboctahedral Pt nanopar-

ticles with Pt-Pt bond lengths from experimental Pt bulk and adsorption energies obtained with geometry optimised Pt nanoparticles. The size effect decreases the Pt-Pt bond lengths, and these deformations change the adsorption energies. The results show that the deformation is not as important as other changes caused by the size effect, with the shifts in adsorption energies being closer or smaller than 0.1 eV in all the cases. Similar results were obtained by other authors when assessing the size effects for O adsorption on edge sites of relaxed and unrelaxed Pt nanoparticles[5].

3 Structural data of adsorbates interacting with isolated Pt nanoparticles

The following table shows detailed structural data regarding the interaction of O, CO, and ethanol with Pt_{13}, Pt_{55}, and Pt_{147} nanoparticles. We present the most stable adsorption site for each adsorbate and Pt nanoparticle size. We show data for CO and ethanol adsorbed at on top sites. For atomic oxygen, we show data about the adsorption at HCP and bridge sites for (111) facets and bridge sites for (100) facets.

Table 1 Structural Parameters of O, CO, and Ethanol adsorbed on Pt nanoparticles. Ethanol values in parentheses were obtained experimentally[6]

Ethanol Adsorption	Pt-O (Å)	C-O (Å)	$_{\alpha}$C-H (Å)	$_{\beta}$C-H (Å)	C-C (Å)	O-H (Å)
Isolated ethanol		1.45 (1.43)	1.10 (1.10)	1.10 (1.09)	1.52 (1.51)	0.98 (0.97)
Top-V Pt_{13} (111)	2.25	1.49	1.10	1.10	1.51	0.98
Top-V Pt_{55} (111)	2.24	1.49	1.10	1.11	1.51	0.98
Top-V Pt_{147} (111)	2.24	1.50	1.10	1.12	1.51	0.98
Top-V Pt_{13} (100)	2.32	1.48	1.10	1.10	1.52	0.98
Top-V Pt_{55} (100)	2.29	1.49	1.10	1.11	1.51	0.98
Top-V Pt_{147} (100)	2.32	1.48	1.10	1.10	1.51	0.98
O Adsorption	Pt-O (Å)					
Bridge-V Pt_{13} (111)	1.99					
Bridge-V Pt_{55} (111)	2.00					
Bridge-V Pt_{147} (111)	2.01					
HCP-V Pt_{13} (111)	2.08					
HCP-V Pt_{55} (111)	2.09					
HCP-V Pt_{147} (111)	2.10					
Bridge-V Pt_{13} (100)	1.97					
Bridge-V Pt_{55} (100)	1.97					
Bridge-V Pt_{147} (100)	1.98					
CO Adsorption	Pt-C (Å)	C-O (Å)				
Isolated CO		1.14				
Top-V Pt_{13} (111)	1.85	1.16				
Top-V Pt_{55} (111)	1.87	1.16				
Top-V Pt_{147} (111)	1.89	1.16				
Top-V Pt_{13} (100)	1.85	1.16				
Top-V Pt_{55} (100)	1.88	1.16				
Top-V Pt_{147} (100)	1.88	1.16				

Table 1 shows all internal bond lengths for each adsorbate and the Pt-O, and Pt-C distances for adsorbates interacting with the Pt nanoparticles. For isolated ethanol, the values obtained in our calculations are comparable with those observed experimentally[6]. Again, for atomic oxygen and carbon monoxide, we observe a small increase in the Pt-O and Pt-C as we increase the nanoparticle size. As discussed in the main article, we see increases in the C-O bond lengths for CO and ethanol, and a small change in the $_{\beta}$C-H bond on ethanol, while other internal bond lengths remained almost constant.

4 Support effect for O, CO, and ethanol for Pt (100) facet

In the main article, we show how the support affects the adsorption properties of Pt nanoparticles interacting with O, CO and ethanol for adsorption sites in the (111) facet. Here, we show similar results obtained when the adsorbates interact with the (100) facet. Again, the Pt nanoparticles are bound to the graphene via the (111) facet. Figure 5 shows how the graphene support changes the interaction between nanoparticles and adsorbates.

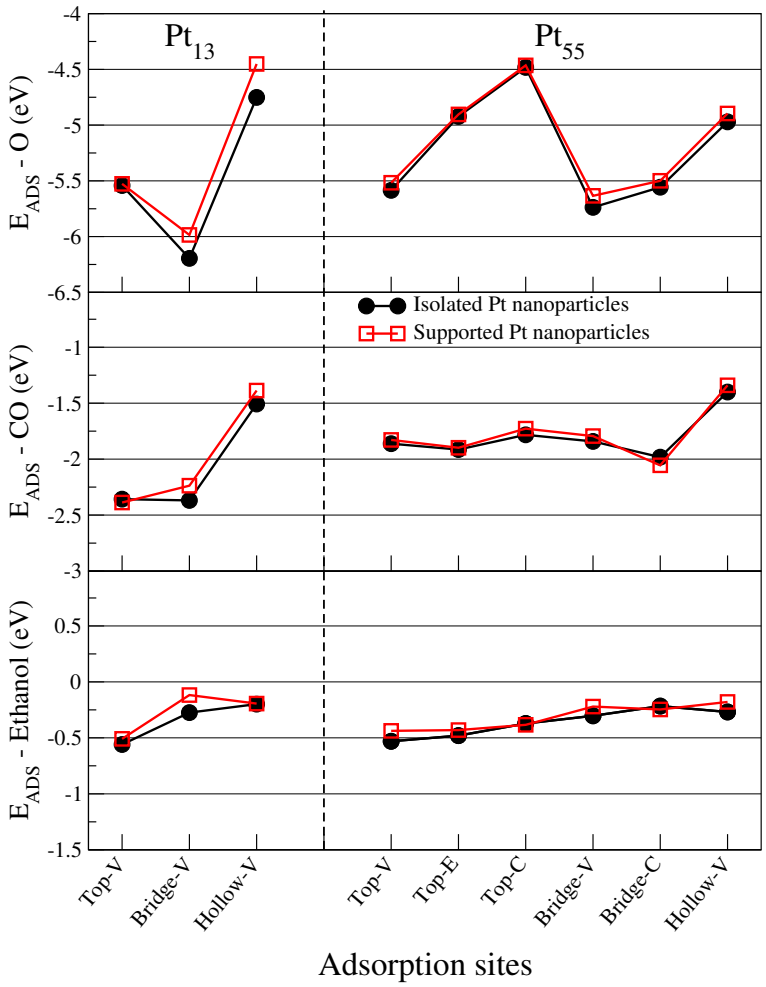

Figure 5 Adsorption energies for oxygen, CO, and ethanol interacting with the (100) facet of Pt_{13}, Pt_{55}, and Pt_{147} on different adsorption sites. The letters V, E, and C represent adsorption sites in the vertex, edge and centre of a nanoparticle facet. Black dots are adsorption energy values calculated for isolated nanoparticles and red open squares are the same values calculated for Pt nanoparticles supported on pristine graphene.

Figure 5 shows that the support effects for adsorption on the (100) facet of the Pt nanoparticles are similar to the ones obtained for (111) facet in the main article. Again, the presence of support weakens the adsorption of O, CO and ethanol on the Pt surface. In all the simulated cases, the change in adsorption energy due to the presence of graphene was lower than 0.3 eV, and the effect of the graphene support decreases as we increase the nanoparticle size. As we observed the same trend in the support effect with increasing nanoparticle size, we decided to avoid calculations with Pt_{147} nanoparticles, as these effects should be negligible.

5 Binding the Pt (100) facet on graphene

The analysis of support effects performed in our paper considered Pt nanoparticles interacting with pristine graphene via the (111) facet. However, we have calculated the adsorption energies for atomic oxygen interacting with adsorption sites on (111) and (100) facets for Pt nanoparticles bound to graphene via the (100) facet.

Paz-Borbón and Baletto[7] recently showed that the adsorption energies of O_2 on PtNi, Pt and Ni nanoparticles can suffer considerable changes when the clusters are bound to MgO supports via the (111) or (100) facets. In our case, the support effect for Pt_{13} interacting with graphene via the (111) and (100) facet is quite similar, being as small as 0.3 eV. For larger clusters, we also see a similar decrease in the support effect with increasing nanoparticle sizes. A possible reason for the similarities between the support effect in both cases could be the weak Pt-graphene interaction, which does not lead to major structural deformations as the ones observed by Paz-Borbón and Baletto[7].

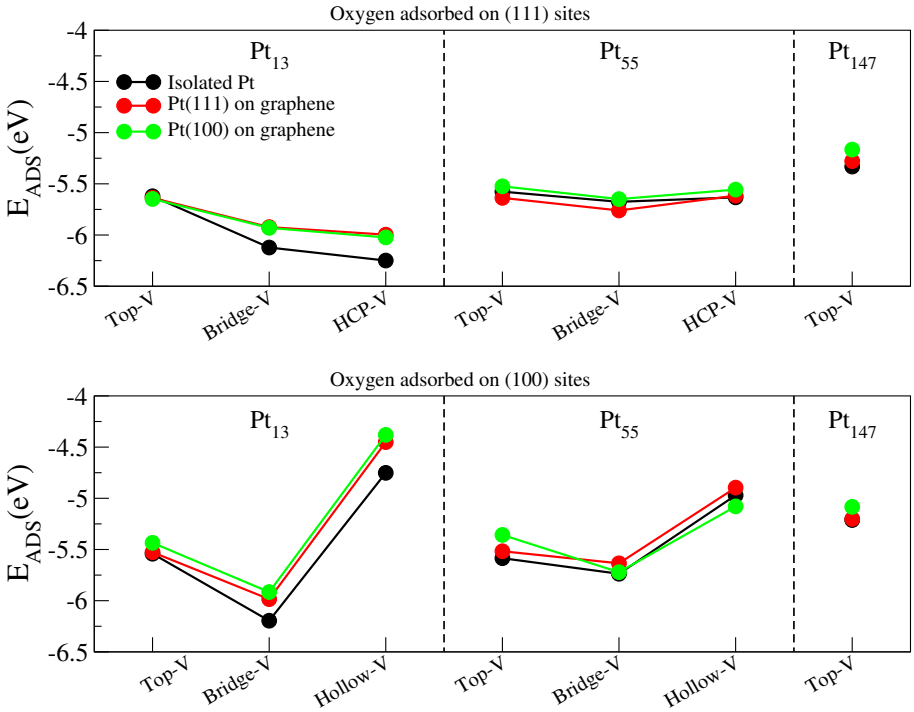

Figure 6 Adsorption energies for oxygen interacting with the adsorption sites in the (111) and (100) facets of Pt_{13}, Pt_{55}, and Pt_{147}, where the letter V represents adsorption sites in the vertices of a nanoparticle facet. Black dots are adsorption energy values calculated for isolated nanoparticles. Red and green dots are the adsorption energies calculated for Pt nanoparticles bound to graphene via the (111) and (100) facet.

6 Generalized coordination number for supported nanoparticles

Figure 7 shows that considerable changes only happen for the adsorption sites on Pt_{13}, which are the three sites with lower generalized coordination numbers. Figure 7 a) shows the data for all the adsorbates and all the adsorption sites calculated for supported and unsupported cases in the main text.

Figure 7 b) shows the results for O adsorption in more details. Considerable changes are only happening for two adsorption sites, and the slope of the linear regression drops from 0.43 eV for isolated nanoparticles to 0.34 eV on supported nanoparticles. These results can be misleading, showing changes in the slopes which are nothing but an

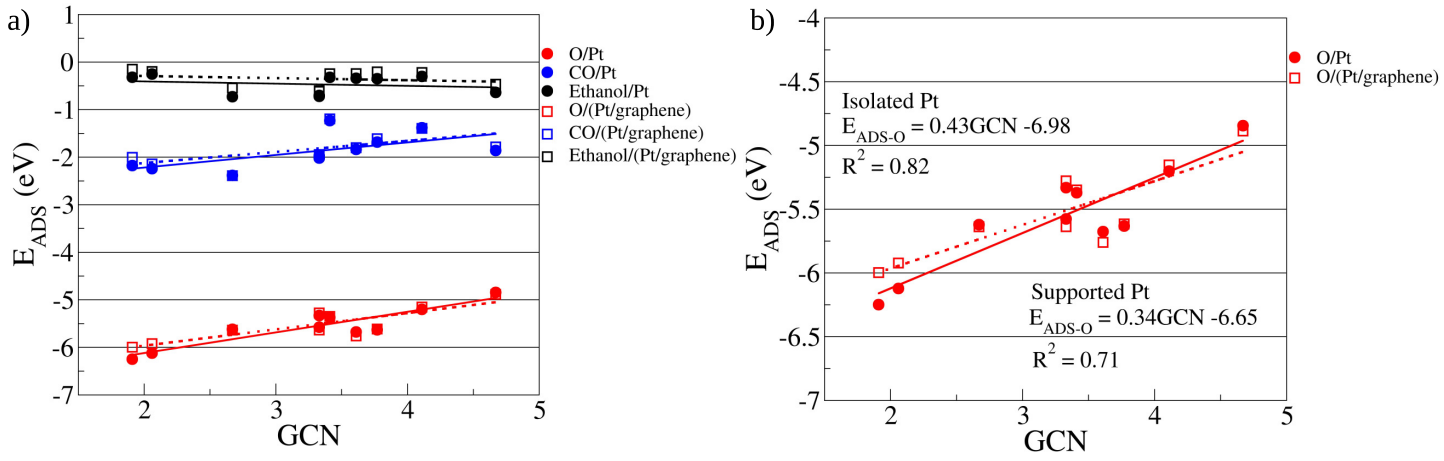

Figure 7 Adsorption energies for O (red), CO (blue) and ethanol (black) on isolated (filled circles) and supported (open squares) Pt nanoparticles. The adsorption sites used for these plots are the ones presented on Figure 8 in the main manuscript. The continuous (segmented) lines are linear regressions obtained for isolated (supported) systems.

artefact caused by the lack of support effects on larger nanoparticles and should not be used to predict the support effect for other nanoparticles and adsorption sites. As an example, one might calculate with these equations that the oxygen adsorption energy for a top site in the centre of a Pt_{309} nanoparticle (GCN=7.5) will be almost 0.2 eV stronger for the supported case, which contradicts the lack of support effects observed for larger nanoparticles.

Thus, to see how the linear dependence of adsorption energies on GCN changes due to the support effects, we believe it is necessary to simulate similar systems on supports with stronger effects, such as metal-oxides or supports with point defects. A support with stronger influence on the nanoparticle would allow assessing these effects on larger nanoparticles with various adsorption sites and draw a better and more reliable correlation about the impact of the support on different adsorption sites.

References

[1] F. Calle-Vallejo, J. I. Martínez, J. M. García-Lastra, P. Sautet and D. Loffreda, *Angewandte Chemie International Edition*, 2014, **53**, 8316–8319.

[2] M. Jørgensen and H. Grönbeck, *ACS Catalysis*, 2017, **7**, 5054–5061.

[3] J. W. Arblaster, *Platinum Metals Review*, 1997, **41**, 12–21.

[4] J. W. Arblaster, *Platinum Metals Review*, 2006, **50**, 118–119.

[5] L. Li, F. Abild-Pedersen, J. Greeley and J. K. Nørskov, *The Journal of Physical Chemistry Letters*, 2015, **6**, 3797–3801.

[6] M. D. Harmony, V. W. Laurie, R. L. Kuczkowski, R. H. Schwendeman, D. A. Ramsay, F. J. Lovas, W. J. Lafferty and A. G. Maki, *Journal of Physical and Chemical Reference Data*, 1979, **8**, 619–722.

[7] L. O. Paz-Borbón and F. Baletto, *Inorganics*, 2017, **5**, 43.